

Molecular characterization and expression of human Rotavirus recombinant protein VP2, VP6, and VP7 transfected in Vero cellLatri Rahmah^{1,2,*}, Ernawati G Rachman², Debbie S Retroningrum², Marselina I Tan²¹ Rotavirus Vaccine Production PT Biofarma, Bandung, Indonesia² Institut Teknologi Bandung, Bandung, Indonesia

Submitted: 21 Nov. 2016; Revised: 9 Feb. 2017; Accepted: 15 Feb. 2017

Abstract

Rotavirus is a non-enveloped viruses containing double-stranded RNA genetic material. The 11 ds-RNA encodes 6 structural and 6 nonstructural proteins. Three major structural capsid proteins of human rotavirus RV4 (VP2, VP6, and VP7) had been isolated, cloned and transfected into Vero cell. VP2 (VP2LRV4), VP6 (VP6LRV4), and VP7 (VP7LRV4) was isolated with the size of coding sequence (CDS) 2673 bp, 1194 bp, and 981 bp, respectively. In silico analysis showed that VP2LRV4, VP6LRV4, and VP7LRV4 protein sequences (prediction) comprised essential subdomain and residues to construct triple layer structural capsid protein. Gene transcription and protein expression of VP2LRV4, VP6LRV4 and VP7LRV4 in Vero cell were examined by RT-PCR and immunofluorescence assay (IF). Transcriptional analysis led to the detection of VP6 and VP7 cDNA on day 1 post transfection while VP2 cDNA was expressed on day 3 post transfection. VP6 and VP7 protein expression marked with fluorescence luminescence in Vero cell on day 1 post transfection.

Keywords: Rotavirus; Vero Cell; VP2; VP6; VP7.**INTRODUCTION**

Rotavirus has been recognized as a major cause of infantile diarrhea in young children. Classify as non-enveloped virus, the genomes of Rotavirus are 11 ds-RNA which encoding 6 structural proteins (VP1-VP4, VP6, and VP7) and 6 nonstructural protein (NSP1-NSP6) (Desselberger, 2014). Rotavirus is composed by three layers (outer, inner and core) capsid protein. In the core site, VP2 is a major protein with VP1 and VP3 as the minor protein. The major capsid protein VP6, which comprises >80% of the protein mass of the particle, is located on the inner capsid and contains the subgroup antigen. The rotavirus outer layer is composed of the glycoprotein VP7 and VP4 (Ruiz *et al.*, 2009).

A number of research reported that the recombinant structural protein of Rotavirus had been expressed in prokaryotic host cell, such as *Escherichia Coli*, and

eukaryotic host cell such as yeast, insect cell, and mammalian cell system. However the expression of recombinant structural protein found several limitations. Rotavirus recombinant protein produce in *Escherichia coli* failed to express and folded properly (Kato *et al.*, 2012). In yeast, it is produced in a lower quantity or inadequate aggregation condition related to glycosylation patterns (Rodriguez-Limas *et al.*, 2011). In Baculovirus system, recombinant Rotavirus protein is degraded and partial loss of ability to form trimmers (Da silva *et al.*, 2012).

Mammalian cells have been chosen as a system for the production of recombinant proteins for its excess on proper protein folding, assembly, and post-translational modification. Vero cells is a mammalian cells that has been widely used for expression recombinant virus protein, such as JEV, PPRV, SV40, rabies, Coronavirus (SARS), Ebola, and Influenza (Hua *et al.*, 2014; Mulherkar *et al.*, 2011; Chen *et al.*, 2011; Siu *et al.*, 2008; Balamurugan *et al.*, 2006; Hsieh *et al.*, 2005; Konishi *et al.*, 2001; Wagner *et al.*, 2000). In the current study, we used Vero cell as mammalian expression system to generate the three major structural recombinant Human Rotavirus RV4 capsid proteins.

***Corresponding author:**

Latri Rahmah, Ph.D.

Rotavirus Vaccine Production PT Biofarma,
Bandung, Indonesia

Email: rahmah_latri@yahoo.com;

latri.rahmah@biofarma.co.id

MATERIALS AND METHODS

Amplification and cloning of VP2, VP6, and VP7 rotavirus gene

Amplification of the complete open reading frame (ORF) of VP2, VP6, and VP7 gene of rotavirus RV4 strain was performed using RT-PCR. Amplification of VP2, VP6, and VP7 were using primer's pair VP2, VP6 and VP7. RT-PCR was performed with an aliquot of dsRNA (100 ng), 4 μ M each of specific primer, 2x Reaction Mix (a buffer containing 0,4mM of each dNTP, 2,4 mM MgSO₄) (Invitrogen) and 1U Super ScriptTM III RT/Platinum Taq High Fidelity Enzyme Mix (Invitrogen) in a final volume 50 μ L. The full-Length VP2 (2.6 kb) cDNA synthesis was obtained by one cycle at 45 °C for 45 min, followed by PCR amplification with 35 cycles at 94 °C for 1 min, 62 °C for 2 min, 72 °C for 2 min and 1 cycle at 72 °C for 7min. The full-Length VP6 (1.3 kb) cDNA synthesis was obtained by one cycle at 45 °C for 45 min, followed by PCR amplification with 35 cycles at 94 °C for 1 min, 47 °C for 2min, 72 °C for 2 min and 1 cycle at 72 °C for 7min. The full-Length VP7 (1 kb) cDNA synthesis was obtained by one cycle at 45 °C for 45 min, followed by PCR amplification with 35 cycles at 94 °C for 1 min, 42 °C for 2min, 72 °C for 2 min and 1 cycle at 72 °C for 7min. The amplified cDNA of VP2 gene was cloned into pCDNA 3.1/TOPO while VP6 and VP7 gene was cloned into pEF6/V5-His-TOPO. Both vectors are dual-host vectors (Invitrogen) for both bacteria and mammalian cells and protein expression in mammalian cells. The recombinant VP2-pCDNA, VP6-pEF, and VP7-pEF was transformed into competent *E.Coli* Top 10 and ampicillin-resistant colonies were screened by ampicillin medium selection. In addition the expected inserts were verified by colony PCR. Colonies PCR were performed using primer's pairs VP2, VP6, and VP7 as described above. Finally, nucleotide sequences analyses were carried out to obtain the full sequences of genes and to confirm the exact in-frame position and correct orientation for subsequent expression.

Protein sequence and structure analysis

Protein sequences (prediction) of VP2, VP6, and VP7 were performed using Bioinformatics tools ExPasy. Three dimensional structures of VP2, VP6, and VP7 were implemented via Phyre2 and Pymol Molecular Graphic System.

Transfection

Vero Cell were seeded at a concentration 1.5 x 10⁴ cells per well in 96-well plates and grown in Opti-MEM for 1 d prior to transfection. To achieve transfection, according to the manufacturer's instruction, 0,2 μ g of Recombinant Vector (pCDNA/VP2, pEF/VP6, pEF/VP7) were mixed with 0.5 μ L lipofectamine

3000TM, 0.4 μ L P3000 reagent, and 10 μ L Opti-MEM (Invitrogen) according to the instruction supplied by the company. Transfection mixture was then added to the seeded cells and incubated at 37 °C from day 1 to 5 for transfection.

RT-PCR analysis

Vero cells transfected with Recombinant Vector (pCDNA/VP2, pEF/VP6, or pEF/VP7) washed two times with PBS and RNA total was extracted by SV Total RNA isolation System (Promega) according to the manufacturer's instruction. The expected fragment of VP2, VP6, and VP7 was amplified by RT-PCR using the primer's pair described above.

Immunofluorescence Assay

Vero cells transfected with Recombinant Vector (pCDNA/VP2, pEF/VP6, or pEF/VP7) fixed in methanol-acetone (1:1) and incubated for 10 m. After fixation, the cells were added by blocking solution (BSA 1%, in PBS-Tween 0.05%) followed with rabbit anti-RV polyclonal antibody (1:800 in PBS). Second-stage antibody was Alexa-488-conjugated secondary antibody diluted at 1:500 in PBS. Cells were examined with a Fluorescence Microscope.

RESULTS AND DISCUSSION

The complete VP2 cDNA sequences (VP2LRV4) with 2679 nucleotides in length contained a 2673 bp CDS that encoded 889 amino acids (Fig. 1A). The complete cDNA sequences (1356 bp) of VP6 (VP6LRV4) comprised an 1194 bp encoding a peptide of 397 amino acids (Fig. 1B). The VP7 sequence (VP7LRV4) was 1062 consecutive bases and contained CDS with 981 bp that encoded 326 amino acids (Fig. 1C). In silico study showed that protein structure (prediction) of VP2LRV4, VP6LRV4, and VP7LRV4 comprised essential subdomain and residues to construct the structural capsid protein (Fig. 2).

The three dimensional structure (prediction) at Figure 2.A showed the dimer domain of VP2LRV4. The dimer subdomain of VP2LRV4 was predicted located in residues 711 to 836 (Fig. 1A). The dimerization of VP2 performed on its dimer domain at residues ~700-826 (Boudreaux *et al*, 2013; McClain *et al*, 2010). Protein structure (prediction) of VP6LRV4 in Fig. 2B showed the domains and residue that was predicted essential to perform trimerization. The essential domain of VP6LRV6 to performed trimerization was predicted located in residues 1 to 150 and residues 151 to 331 (Fig. 1B). Mathieu, *et al* (2001) reported that the VP6 subunit performed trimerization at the domain B (residues 1-150) and domain H (residues 151-331) to construct inner layer Rotavirus capsid protein.

A. VP2LRV4

```

1 ATG GCG TAC AGG AAG CGC GGA GCT AAA CGT GAA AAC TTA CCA CAA CAA AAT GAA CGT CTG CAA GAA AAA GAA ATT GAA AAA GAT GTG GAT GTA ACT ATG GAA AAT AAA AAT AAC AAT AGA AAG CAG CAA TTA TCT 135
136 GAT AAA GTA CTA TCA CAA AAA GAG GAA ATA ATA ACT GAT GCA CAA GAT GAT ATT AAA ATA CGT GGT GAG ATT AAA ACA TCA CCA AAA GAA GAG TCA AAA CAG TTG CTC GAA ATA TTA AAA ACA AAA GAA GAC CAT 270
271 CAG AAA GAA ATA CAG TAT GAT ATT CTA CAA AAA ACG ATA CGC ACT TTT GAA TCC AAA GAA TCA ATT TTG AAA AAA TTA GAA GAT ATA AGA CCG GAG CAA GCT AAG AAG CAA ATG AAA TTG TTT AGA ATA TTT GAA 405
406 CCA AAA CAA TTA CCA ATC TAT CCA GCA AAT GGT GAG AAA GAA TTG AAA AAC AAA TTG AAA AAC GAT ACG CTG CCA GAC GAA TAT GAT GTA CCA GAA TAT TTT AAA TAT TTA TAT GAT CAG 540
541 ATC CTA ATA GAA AAG CAA GAT TTT TTG CTA CCG AAA GAT ACG GCT GTA GAA AAT AAA TCT AGA GAT GCT GGT AAA GTT GTA GAT TCT GAA ACA GCA AAT ATT TGT GAT GCT ATA TTT CAA GAT GAA GAG ACG 585
676 GAG GGA GTT GTC AGA AGA TTC AIT GCA GAT ATG AGA CAA CAG GTT CAG GCT GAT AGA AAT ATT GTC AAC TAT CCA TCA ATT TTA CAT CCG ATT ZAT CAT GCA TTT AAT GAA TAT TTT CAA CAT CAA TTA GTC 720
811 GAA CCA CTA AAT AAT GAA ACT AIT TTT AAT TAT ATA CCA GAA AGA ATA AGG AAT GAT GTT AAC TAT ATT ITG AAT ATG GAT ATG AAT TTG CCA TCA ACA GCA AGA TAT ATT AGA CCA AAT TTA TTG CAA GAT AGA 945
946 CTA AAT TTA CAT GAT AAT TTT GAA TCA TTA TGG GAC ACA ACA ACT ACA TCA AAT TAT ATA CTA GCC AGA TCA GTT GTG CCT GAT TTG AAG GAA AAA GAA TTA GTT TCA ACT GAA GCT CAG ATA CAG AAA ATG TCT 1080
1081 CAA GAT TTG CAA GTT GAA GCG TTA ACG ATA CAA TCT GAA ACG CAG TTT CTT GCT GGC ATA AAT TCA CCA GCA GCA AAT GAT TGT TTT AAA ACA TTG ATA GCA GCT CTG TTA ACG CAG CGT ACA ATG TCA TTA GAT 1215
1215 TTT GTA ACC AGC AAT TAT ATG TCA CTT ATA TCT GGT ATG TGG CTA TTG ACC GTT ATA CCA AAT GAC ATG TTT CTT GGT GAA TCA TTA STC GCA TGC GAA TTG GGC AIA ATA AAT ACT AIA GTT TAT CCA GCA TTT 1350
1351 GAA AIT CAA Agh AIG ATC TAT AGA AAT GGT GAT CCG CAG ACT CCG TTT CAA AIA GCA GAA CAG CAA AIA CAA AAT TTT CAA TCA GCT AAT TGG TTA CAT TTT AAT AAT AAT AGA TTT AGG CAA GTT GTT AIT 1485
1485 GAT GGA GTG TTA AAT CAA CCA CTT AAC GAT AAT AIT AGG AAT GGA CAA GTT AAT AAT CAG TTA ATG GAA GCA TTA ATG CAG CTA TCT AGA CAA CAA TTT CCG ACT ATG CCA GTT GAT TAT AAA ACA TCA ATC CAA 1620
1665 TTA ACA AGA TTA GTA TCA TAT AAT TAT GAA ACT CTA ATG GCT TGT GTA ACT ATG AAT ATG CAA CAT GAT CCA ACT CTC ACT ACC GAA AAA TTA CAA TTA ACT TCT GTC ACA TCT TTA TGT ATG TTA ATT GGA AAT 1800
1801 ACT ACA GTA ATT CCA AGT CCA CAA AIA TTA TTT CAC TAT TAT AAC GTA AAT GTA AAT TTT CAT TCA AAT TAT AAC CAA CGA ATT AAC GAC GCA ZTG GCT ATC AIT ACG GCT GCT ACA ATG AGA CTA AAC TTA CAG 1935
1935 AAA AAA ATG AAA TCA ATA GTT GAG GAT TTT TTG AAA AGA TTG CAA AIT TTT GAT GTA CCA GSA GTA CCA GTA ATA AIT GCT TAT AGA GAT ATG CAA CTA GAA AGA GAT GAG ATG TAT GGA TAT GTC AAT GCT AGA 2205
2071 ATA TTT AAT TTA ATA TTA ATG AAT ATG GAG CAG ATC GAA CCA GCT TCA GAT AAA ATT CCT CCA GSA GTA ATA AIT GCT TAT AGA GAT ATG CAA CTA GAA AGA GAT GAG ATG TAT GGA TAT GTC AAT GCT AGA 2205
Gln Gly Val Ile Ile Ala Tyr Arg Asp Met Gln Leu Glu Arg Asp Glu Met Tyr Gly Tyr Val Asn Ile Ala Arg
Dimer forming subdomain
2205 AAT CTC GAT GGA TAT CAA CAA AtT AAc C7a gaG GAG TTG ACG AGA ACT GGA GAC TAT GGG CAA ATT ACT AAT ATG TTA TTA AAC AAT CAG CCT ZTA GCT TTA GTA GGG GCA TTA CCA TTT GTG ACG GAT TCT TCA 2340
Asn Leu Asp Gly Tyr Gln Gln Ile Asn Leu Glu Leu Met Arg Thr Gly Asp Tyr Gly Gln Ile Thr Asn Met Leu Leu Asn Asn Gln Pro Val Ala Leu Val Gly Ala Leu Pro Phe Val Thr Asp Ser Ser
2341 GTT ATA TCA CTC AIT CCA AAA TTA GAT GCT ACA GTT TTT GCT CAA ATA GTT AAA CTT AGA AAA GAG GAC ACT CTA AAA CCA AIA TTG TAT AAG ATA AAT TCT GAT TCT AAT AAT TTC TAC TTA GTT GCA AAT TAT 2385
Val Ile Ser Leu Ile Ala Lys Leu Asp Ala Thr Val Phe Ala Gln Ile Val Lys Leu Arg Lys Val Asp Thr Leu Lys Pro Ile Leu Tyr Lys Ile Asn Ser Asp Ser Asn Phe Tyr Leu Val Ala Asn Tyr
2475 GAT TGC ATC CCA ACT TCA ACC ACA AAA GTC TAT AAA CAA CCA CCA CAA CCA CTT TTT GAT ATC AGA CCG TCA ATG CAT ATG TTA AGC GCG TCA ATG CAT ATG TTA ACG TCT AAT TTG ACT TTT ACA GTT TAT TCT GAT TTA TTA TCT TTC GTT TCT GCA 2610
Asp Trp Ile Pro Thr Ser Thr Thr Lys Val Tyr Lys Gln
2611 GAC ACG GTT GAA CCC AAT AAC GCA GTT GCT TTT GAC AAT ACG CCG AIT ATG AAC GAA CTG TAA 2673
STOP
    
```

B. VP6LRV4

```

1 ATG GAG GTT CTG TAT TCA TTG TCA AAA ACT CTT AAA GAT CCG AGS GAT AAA AIT GTT GAA GGT ACA CTA TAC TOC AAT GTT AGC GAT CTC AIT CAA CAA TTT AAT CAA ATG ATA GTG ACT ATG AAT GGA AAT GAC 135
1 F V L Y S L S K I L K D A R D K I V E G T L Y S N V S D I Q Q F N Q M I V I M N G N D L 45
Domain B
136 TTT CAA ATG GGA GGA AIT GGT AAT TTA CCT GTT AGA AAT TGG ACT TTT GAT TTT GGT CTA TTA GGT ACA CAA CTT TTA AAT TTG GAT GCT AAT TAT GTT GAA AGT GCA AGA ACT AGT AIT GAA TAT TTC AIT GAT 270
F Q T G G G I G N L P V R N W T F D F L L E T L L L N L D A N Y V E S A R T T I E E Y F I D 90
271 TTT ATC GAT AAC GTA TGT ATG GAT GAA ATG GCA AGA GAG ICT CAA AGA AAT GAA GTA TCA GCT CCA CAA TCT GAA GCG TTG AGG AAG TTA TCA GGC AIT AAA TTT AAG AAG AIA AAT TTT GAT AAT TCA TCA GAA TAT 405
91 F I D N V C M D E M A R E S Q R N G V A F Q S E A L R G K L S G I K F K R I N F D N S S E Y 135
406 ATA GAA AAT TGG AAT CTA CAA AAT AGA AGA CAG CST ACT GTC TTT CAT AAA CCT AAT ATA TTT CCA TAC TCA TCT TCG TTC ACT TTA AAT AGA TCT CCA CAA ATG CAT GAT N L M TTA ATG GGA ACT ATG 540
136 I E N W N L Q N R R Q R T G F Y F L K P N I F P Y S A S F L N R S Q P M H D N L M G T M T 180
Domain H
541 TGG CTT AAT GCT GGA TCA AGA ICA CAA GTC GCT GGT TTT GAT TAT TCA TGT GCT ATA AAG GCA CCA GCA AAT AIC CAG CAG TTC GAA CAT AIT GTG CAG CTT AGA GCT CTA ACT ACA GCT AIT ATA CTG 585
181 W L N A G F D Y I Q V A G F D Y I Q V A C A I N A P A N I A Q Q F E H I V Q L R C A L I T I A I T L 225
676 TTA CCT GAT GCG GAA AGA TTC AGT TTT CCA AGA GTT AAT TCG GCT GAC GSC GCA ACT ACA TGG TTC TTT AAT CCA GTT AIT CTA AGA CCA AAT AAT GTA GAA GTA GAG TTT TTA TTG AAT GGA CAA AIT AIT 810
226 L P D A E R F S F P R V I N S A D G A T T W F F N P V I L R P N N V E V E F L L N G G I I 270
811 AAC ACA TAT CAG GCT ASA TTT GGT ACT AIT ATC CCA AGA AAT TIT GAT ACA AIT C66 TTG TCA TTT CAG TTA ATG C61 CCA AAT ATG ACA CCA GCT GTT AAC GCA TTA TTT CCG CAA C63 CCA CCT TIT CAA 945
271 N T Y Q A R F G T I I A R F D T I R L S F Q P L M R P F A V N A L F A V N A L F Q F Q 315
946 TAC CAT GCA ACT GTT GCA TCA CTA TCA C61 AIT GAT TCT GCT GTC TGC GCA TCA GTG CTT G6G GAG C6G AAT GAA ACT CTG TTA G6S AAT GTG ACT G6G GTA GCT CAA GAT GCT AIA CCA GTT G6A TCA GTA TIT CCA CCA G6C ATG AAT T6G ACT GAG CTA AIT ACT AAC TAT TCA 1125
316 Y H A T V G L T L R I E S A V C E S L A D A N E T L L A N V T A V T A V T A F T G S V 990
991 TGC GAA TCA GTG CTT GCG GAG C6G AAT GAA ACT CTG TTA G6G AAT GTG ACT G6G GTA C61 CAA GAG TAT GCT AIA CCA GTT G6A TCA GTA TIT CCA CCA G6C ATG AAT T6G ACT GAG CTA AIT ACT AAC TAT TCA 1125
C
1126 CCA TCT AGA GAA GAT AAC CTG CAA C6C GTC TTT ACA GTA GCT TCC AIT AGA AGC ATA TTG AIT AAG TGA 1194
    
```

C. VP7LRV4

```

1 ATG TAT GGT AIT GAA TAT ACC ACA AIT CTA ATC TTT CTG ATA TCA ATC AIT CTA CTC AAC TAT ATA CTA AAA TCA GTG ACT C6A ATA ATG GAC TAC AIT ATA TAT AGA TIT TTG TTG AIT TCT GTA CTA TTA TIT 135
1 M Y G I E Y T T I L I F L I S I I L N Y I L V S V T R I M D Y I I Y R F L L I S V A L F 45
136 GCG TTG ACA AGA GCT CAG AAT TAT G6S AIT AAC TTA CCA ATA ACA G6A TCA ATG GAC ACT ACA TAC GCT AIT TTT CTA ACA TCT ACA TTA TGT TIT TAT TCA ACT GAA CCA ACT GAA CCA GAT 270
46 A L T R A Q N Y G I N L P I T I G S M D T A Y A H S T Q E G F L T S T L C L Y V P T E A S I 90
271 ACT CAA AIT AAT GAT G6T GAA TGG AAA GCA TCA TTG TCA CAA ATG TTT CTC ACA AAA GGT TGG CCA ACA GGA TCA GTC VTA TTT AAA GAG TAT TCA AGT AIT GTT GAT TIT TCT GTT GAC CCA CAA TTA TAT TGT 405
91 T Q I N D G E W K D S L S L S Q M F L T I K G W P T G S V Y F K E Y S S I V D F S F Q L Y C 135
406 GAT TAT AAC TTA GTA CTA ATG AAA TAT GAT CAA AAT CTT GAA TTA GAT ATG TCA GAG TTA GCT GAT TTA ATA TIT AAT GAA TGG TTA TGT AAT CCA ATG GAT AIA CCA TTA TAT TAT TAT CAA CAG TCG GGA GAA 450
136 D Y N L V L M K Y D Q N L E L D M S E L A D L I L N E W L C N P M D I T L Y Y Y Q Q S G E 150
541 TCA AAT AAG TGG AIA TCA AGA TCA TCA TGT ACT GTG AAA GTG TGT CCA CTG AAT ACG CAA AGC TTA GGA AIA G6T TGT TGT CAA ACA CCA AAT GAT GAC TCG TIT GAA ATG GTC GCT GAG AAT GAG AAA TTA GCT 585
181 S N K W I S M G S S C T I V K V C P L N T Q T L G I G C Q T T N V D S F E M V A E N E K L A 195
Asn-238
676 ATA GTG GAT GTC GTT GAT G6G AIA AAT CAT AAA AIA AAT TTG ACA ACT ACG ACA TGT ACT AIT C6A AAT TGT AAG AAG TTA G6T CCA GCA GAG AAT GTA GCT AIA GTA CAA GTT GGT GGC TCT AAT TTA GAC 720
226 I V D V V D G E W K I N H K I N L T T T T C T I R N C K K L A G F R E N V A V I Q V F P Q A V N A L F Q F Q 240
Thr-271
811 ATA ACA GCA GAT CCA ACG ACT AAT CCA CAA ACT GAG AGA ATG ATG AGA G6T AAT TGG AAA AAA TGG TGG CAA GTA TIT TAT ACT AIA GTA GAT TAT AIT AAC CAG ACT GTA CAG GTA ATG TCC AAA GAA TCA AGA 855
271 I T A D P T T N P Q T E R M M R V N W K K W Q V F Y T I V D Y I N Q I V Q V M S K R S R 285
946 TCA TTA AAT TCT GCA GCT TIT TAT TAT AGA GTA TAG 981
316 S L N S A A F Y Y R V STOP
    
```

Fig 1: Full nucleotide sequences of VP2LRV4 (A), VP6LRV4 (B), and VP7LRV4 (C).

VP6LRV4 also comprised essential residues 65-LLGTTLL-71, His-153, and Pro-313 (Fig. 1B). Mathieu, *et al* (2001) reported that the VP6 trimmer contained a metal ion that located at the center of the molecule, on the 3-fold molecular axis, coordinated to residue His-153. Previous study had reported the particular segment 65-LLGTTLL-71 of VP6 that facilitated the interaction with VP2 and residue Pro-331 that contacted with residues Pro-279 and Thr-281 of VP7 (Chen *et al*, 2009; Mathieu *et al*, 2001). Fig. 1C showed residues Pro-279, Thr-281, Asn-69 and Asn-238 that were predicted essential in VP7. Chen *et al*,

(2009) reported that residues Pro-279 and Thr-281 of VP7 interact with VP6 protein. The VP7LRV4 also comprised residues Asn-69 and 238 (Fig. 2). Previous study reported that residues Asn-69 and 238 of RV4 were conserved as N-Glycosylated residue (Coulson and Kirkwood, 1991).

The three genes of Rotavirus major structural protein, VP2, VP6, and VP7, have been introduced into Vero Cell using transient transfection. The transient gene expression (TGE) in mammalian cells is configured as an alternative methodology for the rapid production of

recombinant proteins (Jager *et al.* 2007). In this paper, the transient expression of recombinant VP2, VP6 and VP7 of RV4 was described for the first time in Vero cells.

The transcription of VP2, VP6, and VP7 gene in transfectant Vero cells was verified by the RT-PCR analysis. Agarose gel electrophoresis of the RT-PCR products obtained from total RNA extracted from Vero cells that was transfected with the pCMV/VP2, showed expected fragment of 2.6 kb at day 3 post transfection (pt) to day 5 pt (Figure 3). The RT-PCR confirmed that VP2 mRNA was expressed in transfectant Vero cells at day 3 and acquired the highest expression at day 5. These data may indicate that the production of rVP2 protein in Vero cell optimize at day 3 to 5. Several researches also suggest that rVP2 in transfectant cells expressed on day 3 pt (Labbe *et al.*, 1991; Pera *et al.*, 2015; Pourasgari *et al.*, 2007). The RT-PCR assay also confirmed that the VP6 and VP7 mRNA was expressed in transfectant Vero Cell at day 1 to 5 pt. RT-PCR products of Vero cells transfected with the pEF/VP6 or pEF/VP7 were expressed with expected fragment of 1.3 kb and 1.1 kb, respectively (Fig. 3).

Transfected transient cell lines were further examined for the intracellular expression of VP6 and VP7 gene by indirect immunofluorescence assay. As expected, the specific cytoplasmic staining was clearly evident when the transfected cells were reacted with primary polyclonal rabbit anti-rotavirus antibody. The results showed that Vero cells expressed VP6 and VP7 proteins possess a serological specificity similar to that

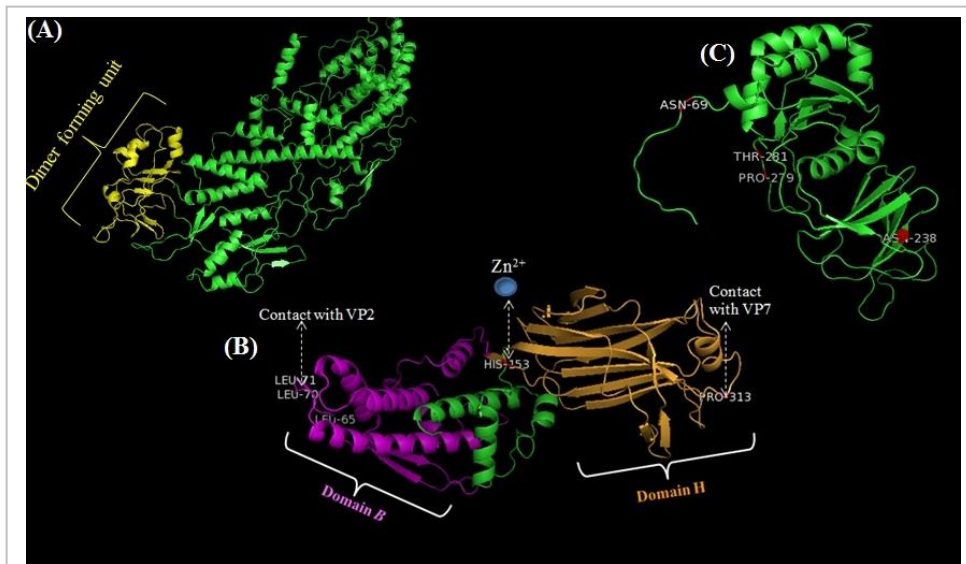


Figure 2: Protein structure (prediction) of VP2LRV4 (A), VP6LRV4 (B), and VP7LRV4 (C). Dimer forming subdomain of VP2LRV4 in yellow. In silico analysis of VP6LRV4 determined domain B in purple (residues 1-150), domain H (residues 151-331) in gold and residue His-153 that essential in the stabilizing the VP6 trimeric molecule. The VP6LRV4 also contained residues 65-LLGTTLL-71 and Pro313 that may contact with VP2 and VP7. VP7LRV4 contained the conserved N-Glycosylated (Asn-69 and 238) and residues Pro-279 and Thr-281 that may interact with VP6.

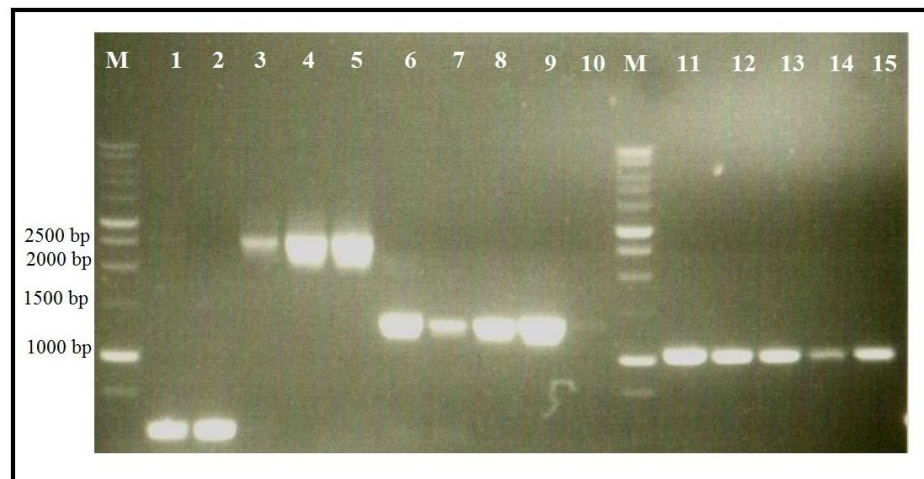


Figure 3: Agarose gel electrophoresis of the RT-PCR products obtained from total RNA extracted from Vero cells transfected with the pCMV/VP2, pEF/VP6, and pEF/VP7 genes. Lanes L: 1kb ladder; Lanes 1 to 5: RT-PCR product of VP2 at 1d to 5d post-transfection; Lanes 6 to 10: RT-PCR product of VP6 at 1d to 5d post-transfection; Lanes 11-15: RT-PCR product of VP7 at 1d to 5d post-transfection

of the viral VP6 and VP7. Our result shows that the transfected Vero cell expressed VP6 and VP7 protein at day 1 to 5 pt (Fig. 4). Interestingly, we observed that the Vero cells transfected with VP7 shows the fluorescence cell with a cell nucleus that more obvious than in the Vero cells transfected with VP6. VP7 is translated at the ribosomes which bind to the membranes of organelles ER while VP6 is translated in polyribosome (Desselberger, 2014). ER membrane lies

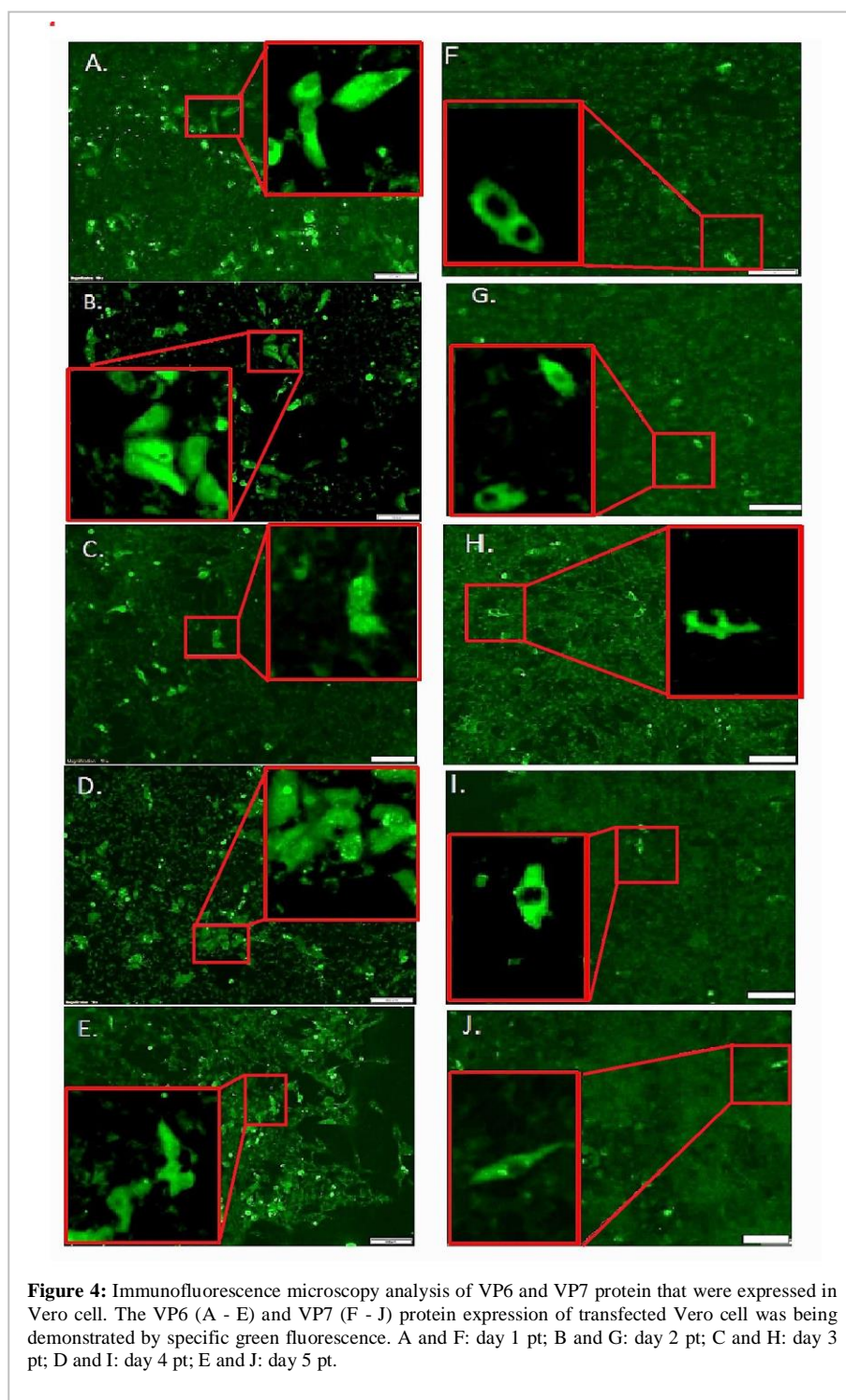


Figure 4: Immunofluorescence microscopy analysis of VP6 and VP7 protein that were expressed in Vero cell. The VP6 (A - E) and VP7 (F - J) protein expression of transfected Vero cell was being demonstrated by specific green fluorescence. A and F: day 1 pt; B and G: day 2 pt; C and H: day 3 pt; D and I: day 4 pt; E and J: day 5 pt.

adjacent to the nucleus while polyribosome scattered in the cytoplasm. Those differences may lead to differing form of fluorescence in transfected cell.

CONCLUSION

The three major structural capsid proteins VP2, VP6, and VP7 of human rotavirus RV4 had been isolated and expressed in Vero cell. In silico analysis showed that

the VP2LRV4, VP6LRV4, and VP7LRV4 protein sequences (prediction) comprised essential subdomain and residues to construct triple layer structural capsid protein. Transcriptional analysis confirmed that the VP2 gene was expressed at day 3 post transfection while VP6 and VP7 were expressed at day 1 post transfection. VP6 and VP7 protein expression in transfected Vero cell occurred on day 1 post single transfection. All of it suggested that this study can be developed as a reference on producing triple layer VLP consist of VP2, VP6, and VP7 in Vero cell.

Conflict of interest

The authors declare no conflict of interest with respect to the content and writing of the paper.

Acknowledgement

This work was funded by PT Biofarma, Indonesia and was carried out in partial fulfillment of PhD thesis supported by School of Life Sciences, ITB.

References

- Balamurugan V, Sen A, *et al.* (2006) Development and characterization of a stable Vero cell line constitutively expressing peste des petits ruminants virus (PPRV) hemagglutinin protein and its potential use as antigen in enzyme-linked immunosorbent assay for sero surveillance of PPRV, *Clin. Vaccine Immunol.*, **13**(12): 8036-8048.
- Boudreaux CE, Vile DC, *et al.* (2013) Rotavirus core shell subdomains involved in polymerase encapsidation into virus-like particles. *J. Gen. Virol.*, **94**: 1818-1826.
- Chen Y, Guo W, *et al.* (2011) A novel recombinant pseudorabies virus expressing parvovirus VP2 gene: immunogenicity and protective efficacy in swine. *Virol J.*, **8**: 307-315.
- Chen JZ., Settembre EC, *et al.* (2009) Molecular interaction in rotavirus assembly and uncoating seen by high-resolution cryo-EM. *PNAS*, **103** (26): 10644-10648.
- Coulson BS, Kirkwood C., (1991) Relation of VP7 amino acid sequence to monoclonal antibody neutralization of rotavirus and rotavirus monotype. *J. Virol.*, 5968-5974.

Human Rotavirus recombinant protein expression in Vero cell

Da Silva Junior HC, Mouta Junior SS, *et al.* (2012) Comparison of two eukaryotic systems for the expression of VP6 protein of rotavirus specie A: transient gene expression in HEK293-T cells and insect cell-baculovirus system. *Biotechnol. Lett.*, **34**: 1623–1627.

Desselberger U (2014) Rotaviruses. *Virus Res.*, **190**: 75-96.

Hsieh PK, Chang SC, *et al.* (2005) Assembly of severe acute respiratory syndrome coronavirus RNA packaging signal into virus-like particles is nucleocapsid dependent. *J. Virol.*, **79**(22): 13848-13855.

Hua, RH, Li, YN, *et al.* (2014) Generation and characterization of new mammalian cell line continuously expressing virus-like particle of Javanese encephalitis virus for a subunit vaccine candidate. *BMC Biotechnol.*, **14**: 62-69.

Jager, V, Bussow K, *et al.* (2015) Transient recombinant protein expression in mammalian cells. *Animal Cell Culture, Cell Engineering 9*. Springer International Publishing, ISBN: 978-3-319-10319-8, **12**: 27-63.

Kato T, Deo VK, *et al.* (2012) Functional virus-like particles production using silkworm and their application in life science. *J. Biotechnol. Biomaterial*, S9:001, doi:10.4172/2155-952X.S9-001.

Konishi E, Fujii A, *et al.* (2001) Generation and characterization of a mammalian cell line continuously expressing japanese encephalitis virus subviral particles. *J. Virol.*, **75** (5): 2204-2212.

Labbe M, Charpilienne A, *et al.* (1991) Expression of rotavirus VP2 produces empty core like particles. *J. Virol.*, **65** (6): 2946-2952.

Mathieu M, Petitpas I, *et al.* (2001) Atomic structure of the major capsid protein of Rotavirus: implication for the architecture of the virion. *EMBO J.*, **20**(7): 1485-1497.

McClain B, Settembre E, *et al.* (2010) X-Ray Crystal structure of the Rotavirus inner capsid particle at 3.8 Å resolution. *J. Mol. Biol.*, **397**: 587-599.

Mulherkar N, Raaben, M, *et al.* (2011) The ebola virus glycoprotein mediates entry via a non-classical dynamin-dependent macropinoscytic pathway. *Virology*, **419**: 72–83.

Pourasgari, Ahmadian, S, *et al.* (2007) Expression and characterization of VP2 protein of human rotavirus a in a mammalian lung cell line. *Acta Virol*, **51**: 261 – 264.

Pera FFPG, Mutepfa DLR, *et al.* (2015) Engineering and expression of a human rotavirus candidate vaccine in *Nicotiana benthamiana*. *Virol J.*, **12**: 205-211.

Ruiz MC, Leon T, *et al.* (2009) Molecular biology of rotavirus entry and replication, *Sci. World J.*, **9**, 1476–1497.

Rodríguez-Limas WA, Tyo KE, *et al.* (2011) Molecular and process design for rotavirus-like particle production in *Saccharomyces cerevisiae*. *Microb Cell Fact.*, **10**: 33-43.

Siu YL, Teoh KT, *et al.* (2008) The M, E, and N structural proteins of the severe acute respiratory syndrome coronavirus are required for efficient assembly, trafficking, and release of virus-like particles. *J. Virol.*, **82**(22): 11318–11330.

Wagner E, Engelhardt OG, *et al.* (2000) Formation of virus-like particles from cloned cDNAs of togoto virus. *J. Gen. Virol.*, **81**: 2849–2853.